217. Reaction Rates of *t*-Butyl and Pivaloyl Radicals in Solution

by **Hans Schuh, Edwin J. Hamilton, Jr.**[1]**, Henning Paul** and **Hanns Fischer**

Physikalisch-Chemisches Institut der Universität Zürich, Rämistrasse 76, CH–8001 Zürich

(8. VII. 74)

Summary. The rate constants of the unimolecular decomposition of the pivaloyl radical (k_D) and of the bimolecular self terminations of pivaloyl (k_1) and *t*-butyl radicals (k_2) in liquid methylcyclopentane are determined by ESR.-spectroscopy:

$$\log (k_D/s^{-1}) = 11.9–9.3/\Theta$$
$$\log (k_1/M^{-1}\,s^{-1}) = 13.0–3.6/\Theta$$
$$\log (k_2/M^{-1}\,s^{-1}) = 11.2–2.0/\Theta$$

The viscosity dependence of k_2 is analysed with respect to diffusion control of the reaction. Comparison of k_D values of different acyl radicals reveals a strong dependence of the activation energies on radical structure.

1. Introduction. – Electron spin resonance (ESR.) spectroscopy of transient radicals during fast photochemical or thermal reactions allows the identification of the reaction intermediates, their reactions and the determination of absolute reaction rates [1]. Recently, several groups of authors have applied ESR. in studies of rate constants of self termination [1–6] and addition reactions [7] of photochemically produced radicals and have published suitable experimental techniques involving time dependent radical generation [8] [9]. The studies were limited to small temperature ranges and few activation parameters were reported.

In this paper, we extend our previous studies of photochemically produced radicals and their reaction rates [10–12] to a determination of the absolute rate constants of self termination of the pivaloyl ($R^1 = (CH_3)_3C\dot{C}O$) and *t*-butyl ($R^2 = (CH_3)_3C\cdot$) radicals and of decomposition of pivaloyl ($R^1 \rightarrow R^2 + CO$) in a wide temperature range. The radicals are produced by photocleavage of di-*t*-butylketone in methylcyclopentane solutions. Steady state and time resolved ESR.-spectroscopy is applied.

The particular chemical system was chosen for several reasons: Firstly, the radical reactions are rather simple and well known at room temperature [13] [14]. Secondly, the high quantum yield of cleavage leads to strong ESR.-signals of R^1 and R^2 [10] [11]. Thirdly, though the self termination of *t*-butyl (R^2) has been reported for several systems at or near room temperature [3] [5] [12] [15] the data show a considerable scatter and no activation parameters have been given. These would be highly instructive with respect to the possible diffusion control of this reaction in solution and for a comparison with the recent gas phase values [16]. Finally, the rate constant for decomposition of pivaloyl, a reaction reported for liquids [17], is of interest because a comparison with the known constants of other

[1] Present adress: Argonne National Laboratory, Argonne, Ill. 60439.

acyl radicals [18–20] should reveal the dependence of decomposition rates on radical structure.

In the following steady state ESR.-techniques are applied for the temperature range $-120° \leq T \leq -10°$ to determine the relative rates of self termination of R^1 and R^2 and of decomposition of R^1. Time resolved ESR.-spectroscopy is used in the high temperature range of fast decomposition of R^1, $-7.5° \leq T \leq +40°$, for a determination of the absolute rate of self termination of R^2. Combination of the results leads to the absolute rates of all the reactions and their activation parameters. In some experiments benzene is used as solvent instead of methylcyclopentane.

2. Solution photochemistry of di-*t*-butylketone and radical reaction kinetics. – Alkane or methylenechloride solutions of di-*t*-butylketone show a $n\pi^*$-absorption band in the region 245 nm $\leq \lambda \leq$ 325 nm (ε(Max) = 21 M^{-1} cm^{-1} at λ = 295 nm in methylenechloride). UV.-absorption in this region at room temperature leads for alkane and benzene solutions to the formation of the major products carbon monoxide, isobutane, isobutene and hexamethylethane and small amounts ($\leq 5\%$) of pivalaldehyde [13] [14]. As evident from previous studies [10] [13] [14] [21] [22] the reactions involve photocleavage of the ketone predominantly from the $n\pi^*$-triplet state with a quantum yield of 0.71 and subsequent reactions of the primary pivaloyl and *t*-butyl radicals. Reactions (1) to (7) account for all the products and occur also in the gas-phase photolysis [23] [24] (R = $(CH_3)_3C$).

$$R - CO - R \xrightarrow{h\nu,\ I} \underset{(R^1)}{R - \dot{C}O} + \underset{(R^2)}{R\cdot} \qquad (1)$$

$$R^1 \xrightarrow{k_D} R^2 + CO \qquad (2)$$

$$2\,R^2 \xrightarrow{k_2(d)} R(+H) + R(-H) \qquad (3)$$

$$\xrightarrow{k_2(c)} R - R \qquad (4)$$

$$R^1 + R^2 \xrightarrow{k_x(d)} R - CHO + R(-H) \qquad (5)$$

$$\xrightarrow{k_x(c)} R - CO - R \qquad (6)$$

$$2\,R^1 \xrightarrow{k_1(c)} R - CO - CO - R \qquad (7)$$

At room temperature the decarbonylation of R^1(2) occurs faster than termination (5)–(7) since more than 95% of the ketone is transformed to CO and the products of reactions (3) and (4), the formation of pivalaldehyde and the regeneration of the ketone are low, and R^2 is the only radical observed by ESR. [10] [11] [13] [14]. At low temperatures R^1 can also be observed and a semidione type radical is found which arises by a photoreaction of the primary dione (7) with the solvent [10]

$$R - CO - CO - R + SH \xrightarrow{h\nu} R - \dot{C}OH - CO - R + S\cdot \qquad (8)$$

This indicates that the decarbonylation (2) competes with radical termination at low temperatures and must be a highly activated process.

Our analysis of radical concentrations of R^1 and R^2 will be based on the reactions (1) to (7). We neglect reaction (8) since the concentration of the semidione radical R^3 was always found to be very small. Further, we do not consider reactions of R^1 or R^2 with the solvent or the ketone since no radicals nor products of such reactions were observed. Also, the reversion of reaction (2)

$$R^2 + CO \rightarrow R^1 \tag{9}$$

is not taken into account since conversion of the ketone and thus CO production was low. The terminations (3) and (4) of R^2, (5) and (6) of R^1 and R^2 and (7) of R^1 are described by the gross rate constants, $k_1 = k_1(c)$, $k_x = k_x(c) + k_x(d)$ and $k_2 = k_2(d) + k_2(c)$, respectively. Thus, the rate equations for the concentrations of R^1 and R^2 become

$$\dot{c}_1 = I - 2k_1 c_1^2 - k_x c_1 c_2 - k_D c_1 \tag{10}$$

$$\dot{c}_2 = I - 2k_2 c_2^2 - k_x c_1 c_2 + k_D c_1 \tag{11}$$

where I is the rate of reaction (1). For continuous photolysis (I = const.) we obtain with the usual assumption $k_x = 2(k_1 k_2)^{1/2}$ [25] for the steady state radical concentrations ($\dot{c}_1 = \dot{c}_2 = 0$)

$$2k_1^{1/2} c_1 = I^{1/2} \left\{ 1 - \frac{k_D}{k_D + 2(k_1 I)^{1/2}} \right\}, \tag{12}$$

$$2k_2^{1/2} c_2 = I^{1/2} \left\{ 1 + \frac{k_D}{k_D + 2(k_1 I)^{1/2}} \right\}. \tag{13}$$

These relations show that for negligible decomposition of R^1 ($k_D \approx 0$), c_1 and c_2 should both depend linearly on the square root of the initiation rate, *i.e.* the light intensity, and should be related by

$$c_2/c_1 = (k_1/k_2)^{1/2}. \tag{14}$$

For intermediate decomposition ($k_D \approx 2(k_1 I)^{1/2}$) negative ($c_1$) and positive ($c_2$) deviations from the linear dependencies on $I^{1/2}$ are expected, whereas for fast decomposition ($k_D \gg 2(k_1 I)^{1/2}$) $c_1 = 0$ and $(k_2)^{1/2} c_2 = I^{1/2}$.

For intermittent photolysis (I = I in the on-period, I = 0 in the off-period) at high temperatures ($k_D \gg 2(k_1 I)^{1/2}$) (10) and (11) lead to the time dependence of c_2 in the off-period ($t \geq 0$)

$$\frac{c_2(t)}{c_2(0)} = (1 + 2k_2 c_2(0) \cdot t)^{-1}. \tag{15}$$

In section 4 we determine the low temperature region of neglegible decomposition by a study of the dependencies of c_1 and c_2 on the light intensity and obtain k_1/k_2 from the radical concentrations in this region by Eq. (14). $2k_2$ is obtained at temperatures of fast decomposition by time resolved studies according to (15). Extrapolation to the low temperature region yields k_1 and analysis of the concentrations in the intermediate region by (12) and (13) leads to k_D.

3. Experimental Part. – Much of the experimental arrangement was similar to that used in earlier steady state and kinetic experiments [10–12]. The di-*t*-butylketone solutions were freed from dissolved oxygen by purging with helium and were then passed from a syringe through a flat reaction cell. The cell is part of a dewar arrangement located in the part of a double cavity which is next to the irradiation window (80% transmission). The rear part of the cavity contained a stable standard sample (*Varian* strong pitch) for calibration purposes. Flat cells of optical path

lengths of 0.44 mm and 0.63 mm were used, ketone concentrations being 3% by volume for the 0.44 mm and 2% by volume for the 0.63 mm cell. They lead to absorbances less than 30% in the whole $n\pi^*$-transition region. The flow rate was 0.4 cm³/min, and conversion of ketone was less than 20%.

The sample temperature was varied by passing a stream of temperature controlled nitrogen gas over the cell [10] and was measured by a thermocouple in the liquid above the irradiation zone. Temperatures given below are accurate to $-1°$ and $+3°$.

The UV.-source was an air-cooled 1 kW-Hg-Xe high pressure lamp (*Hanovia* 977 B-1) mounted in a housing for optimum horizontal light output [8]. This lamp and the horizontal arrangement was preferred over the previously used source [10] because it provides a more stable light beam. By filtering with nickel/cobalt sulfate solutions [10] and UV.-transparent glasses (UG 11, *Schott* und *Gen.*) the wavelength range for photolysis was limited to $265 \leq \lambda \leq 340$ nm in steady state experiments. In time resolved studies the range was $225 \leq \lambda \leq 340$ nm. In all experiments particular attention was paid to ensure a homogenous light intensity distribution over the whole area of the flat cell. This was achieved by optimizations of the beam geometry based on visual observation of the fluorescence of anthracene solutions in the sample cell. We have found that inhomogeneous intensity distributions may lead to large errors in radical concentrations if the usual calibration procedure of relating the ESR.-signal intensity of the sample to that of a standard sample with homogeneous radical distribution is applied. In particular, optimization for largest ESR.-signal implies focussing the beam to the most sensitive center part of the cavity and leads to overestimates of radical concentrations and correspondingly to too low reaction rate constants.

In the steady state experiments the light was transmitted to the sample cell by two suprasil lenses without intermediate focussing. The light intensity was varied by insertion of discs with holes calculated to give the desired transmission $f = I/I_0$. The transmissions were further calibrated by control experiments with a linear photoelement at the position of the sample cell.

The arrangement for time resolved studies involved intermediate focussing of the light beam on a slot (5×12.5 mm) where it is chopped by a rotating sector (diameter 200 mm, one on/off-period, on: off-ration 1:3). The sector is mounted on the shaft of a motor (*Minarik NSE-13*) with variable revolution frequency ($0 \leq \nu \leq 200$ s^{-1}, with sector). Normally frequencies of 180–200 s^{-1} were applied, corresponding to sector errors of about 50 μs. A block diagram of the arrangement is shown in Fig. 1. The details of data and baseline acquisition (acquisition time per data point 40 μs) by computer control have been described previously [12]. In the present study we have further checked that variations of sector frequency in the range $165 \leq \nu \leq 200$ s^{-1} and of the initial concentration c_2 (0) by a factor of 2 were without influence on the observed reaction rate constants.

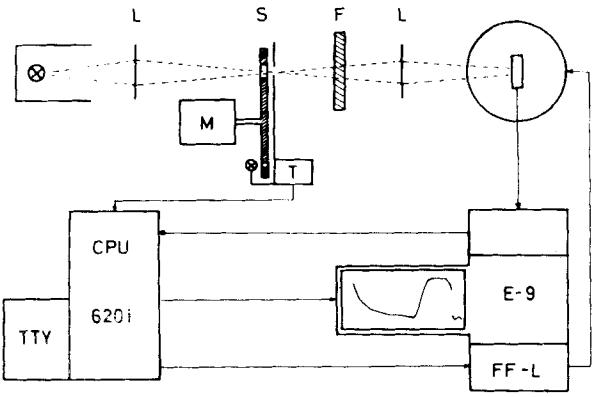

Fig. 1. *Arrangement for kinetic ESR.-spectroscopy.* L: lenses, F: filtersystem, S: sector, M: motor, T: trigger, CPU: computer and interface, *Varian* 620i, TTY: teletype, E-9: ESR.-spectrometer, FF-L: field frequency lock system

Absolute radical concentrations were determined by relating the areas of the ESR.-absorption curves of R^1 and R^2 to those of solutions of the stable radicals α, α-diphenyl-β-picrylhydrazyl and galvinoxyl, the amplitude of the substandard in the double cavity serving as internal reference. The calibration of the internal reference was carried out at room temperature. Since in actual experiments R^1 and R^2 were measured at various temperatures and with different spectrometer setting the *Curie*-correction was taken into account and the dependencies of the signals on microwave power, modulation amplitude and receiver gain were determined and accounted for. Further a slight ESR.-polarization of R^2 leading to larger intensities on the high field side of the spectrum than on the low field side was found and corrected for by assuming that positive contributions on the high field side cancel the negative contributions on the low field side as it has been observed for other radicals [26] [27]. All area determinations were carried out by computer double integrations of noise free derivative lines simulated to give a best fit to the experimentally observed lines. We believe that the absolute radical concentrations and rate constants given below are accurate to ± 40%, relative errors being of the order of about ± 20%.

Methylcyclopentane and di-*t*-butylketone were purchased from *Fluka*, *Pfaltz & Bauer* and *Merck* in the purest available form. NMR.-, UV.- and GC.-analysis revealed no disturbing impurities. We thank *P. Vesel* for the preparation of 2,2,5,5-tetramethylhexane-3,4-dione and for determinations of viscosities by *Ostwald*-viscosimetry.

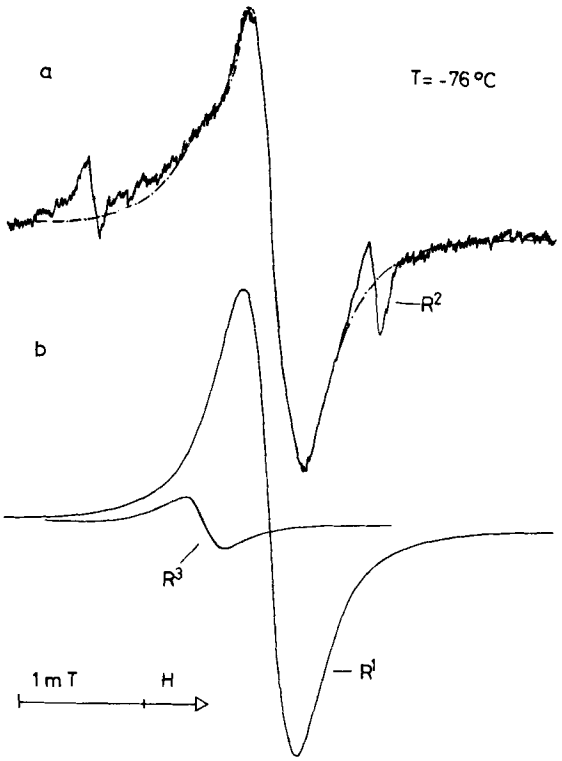

Fig. 2. *ESR.-spectrum of* R^1, R^2, R^3: a) experimental; b) simulated spectra of R^1 and R^3; broken line: superposition of the spectra of R^1 and R^3

4. Results. – The ESR.-spectra of *t*-butyl (R^2) and pivaloyl (R^1) in methylcyclopentane have been reported previously [10]. R^2 shows 10 groups of lines with fully resolved second order structure. The line width of the individual components

($8 \cdot 10^{-3}$ mT) was independent of temperature and probably governed by magnetic field inhomogeneity. The maximum in the saturation curve is found at an incident microwave power of about 1 mW. R^1 exhibits a single broad line at $g = 2.0008$ with a peak to peak line width increasing linearly with temperature (0.37 mT at 163 K, 0.80 mT at 263 K). No indications of saturation can be found for microwave powers less than 400 mW. Fig. 2a shows the center portion of a spectrum taken with high microwave power at $T = -76°$. Besides the two saturation broadened center line groups of R^2 it exhibits the broad singlet attributed to R^1. Careful analysis shows that the low field shoulder of the signal of R^1 carries an additional singlet R^3 and part b of the Figure displays the contributions of R^1 and R^3 to the experimentally observed singlet. R^3 is identified as $(CH_3)_3CCOCOHC(CH_3)_3$ because its signal ($g = 2.0044$) is identical to that of the authentical semidione radical generated by photoreduction of 2,2,5,5-tetramethylhexane-3,4-dione in the same solvent and for identical temperature and spectrometer conditions. Further, its signal increases with increasing ketone conversion. We believe that R^3 is formed via reaction (8).

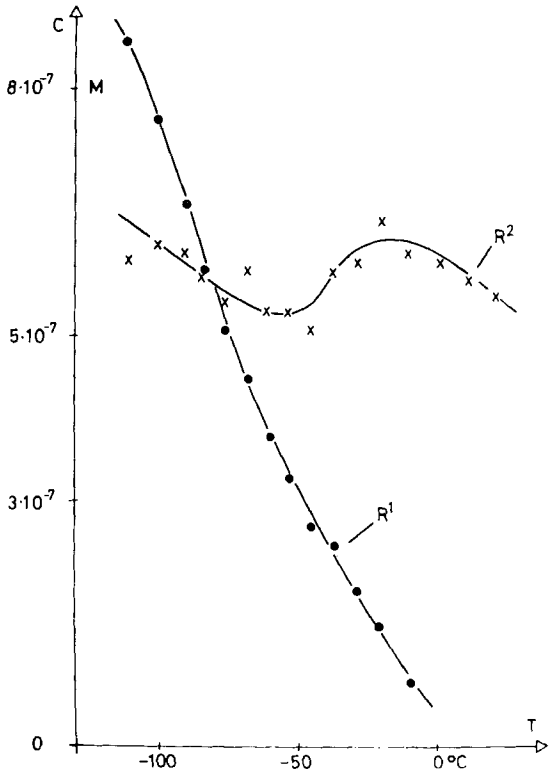

Fig. 3. *Absolute concentrations of R^1 and R^2*

Fig. 3 shows the absolute concentrations of R^1 and R^2 as functions of temperature. Whereas the concentration of R^1 strongly decreases with increasing temperature R^2 increases in concentration for $-60° \leq T \leq -30°$. These findings are interpreted as

follows: For $T \lesssim -70°$ decarbonylation of R^1(2) is slow compared to termination, the decreases of the radical concentrations being due to a slight activation of the termination reactions (3) to (7). For $-70° \lesssim T \lesssim -10°$ decarbonylation competes with terminations, and for $-10° \lesssim T$ decarbonylation is fast compared to the terminations. The decrease of the concentration of R^2 at high temperatures is again ascribed to an activation of termination reactions (3) and (4). As outlined in section 2 the results of Fig. 3 were expected from earlier findings.

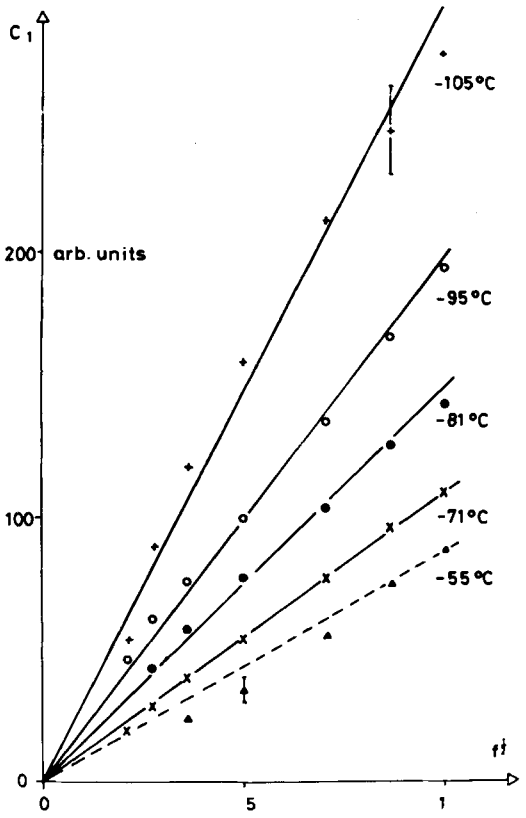

Fig. 4. c_1 *versus* $f^{1/2}$

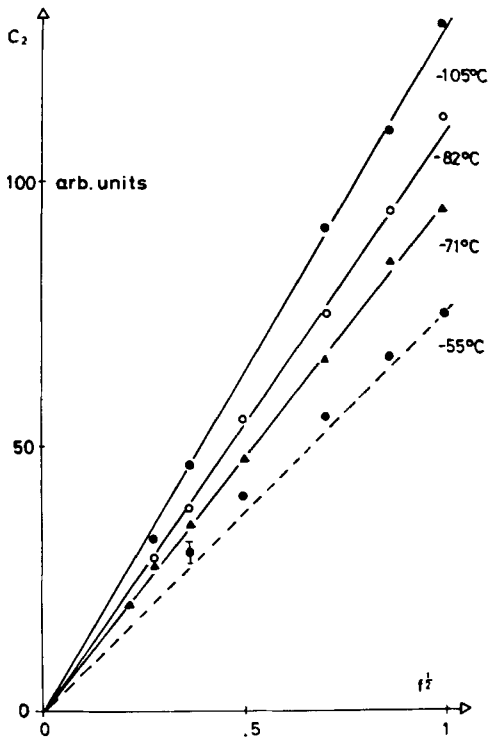

Fig. 5. c_2 *versus* $f^{1/2}$

If our analysis is correct the concentrations of R^1 and R^2 should depend linearly on the square root of the light intensity for $T \lesssim -70°$. As Fig. 4 and 5 demonstrate this is indeed observed. These figures also show the expected deviations for a temperature of intermediate decarbonylation following from Eq. (12) and (13). From the radical concentrations for $T < -70°$ we obtain the ratio k_1/k_2 by applying Eq. (14). An *Arrhennius* plot of this ratio is given in Fig. 6. It indicates a difference in activation energies $E_1 - E_2 = 6.7$ kJ/mol $= 1.6$ kcal/mol.

The absolute termination rate constant k_2 of *t*-butyl (R^2) was determined in the temperature range of fast decarbonylation ($-7.5° \leq T \leq 46°$) by the time resolved method. The spectrometer was set to a magnetic field position corresponding to the

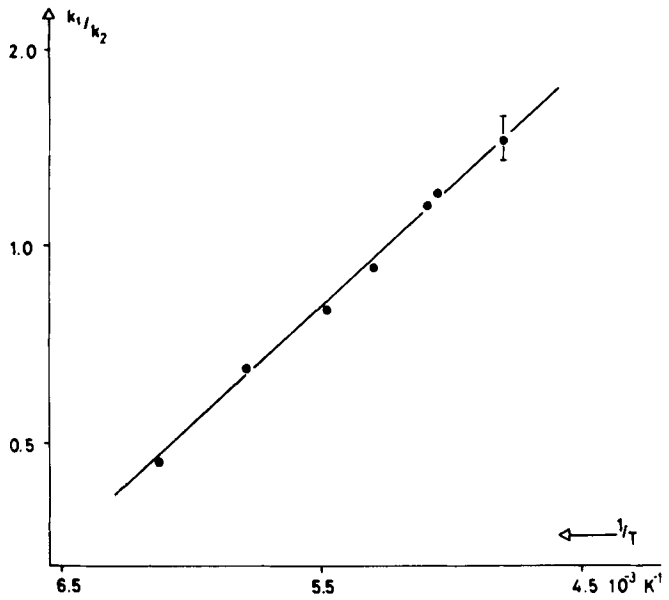

Fig. 6. Arrhennius *plot* k_1/k_2

most intense line of the second order groups. Fig. 7 shows the experimental time dependence of c_2 starting with an interrupt of irradiation at $t = 0$. The baseline of the spectrometer $c_2 = 0$ is also given. The dotted curve represents a computer generated best fit of the decay curve to Eq. (15). The region of fitting is indicated by arrows. From the fitting parameter $2k_2c_2(0)$ we obtain $2k_2$ by a calibration of $c_2(0)$, and an *Arrhennius* plot of $2k_2$ is given in Fig. 8. The straight line is a best fit to the experimental values. Extrapolating k_2 to the low temperature region we obtain k_1 from Fig. 6. The decarbonylation constant k_D is then found by analysis of the radical concentrations in the intermediate temperature range ($-70° \lesssim T \lesssim -10°$) by Eq.

Fig. 7. *Time dependence of* c_2

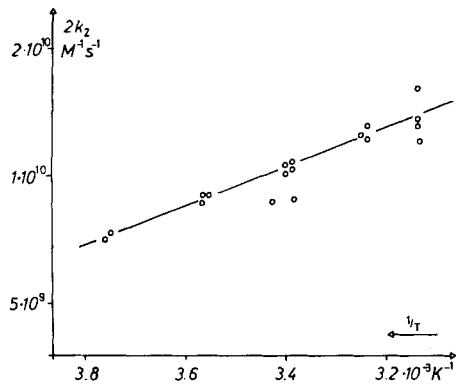

Fig. 8. Arrhennius *plot of* $2k_2$

(13) and (14). Further the rate of initiation follows from the data of Fig. 3 by use of (10) and (11) with $\dot{c}_1 = \dot{c}_2 = 0$. *Arrhennius* plots of k_D and I are given in Fig. 9 and 10. The excellent straight line behaviour of both quantities support the validity of our extrapolation procedure. The final results are

$$\log (k_1/M^{-1}\,s^{-1}) = 13.0 - \frac{3.6}{\Theta}$$

$$\log (k_2/M^{-1}\,s^{-1}) = 11.2 - \frac{2.0}{\Theta}$$

$$\log (k_D/s^{-1}) = 11.9 - \frac{9.3}{\Theta}$$

$$\log (I/M\,s^{-1}) = -1.6 - \frac{1.2}{\Theta}$$

where $\Theta = 2.303\ RT$, expressed in kcal/mol.

5. Discussion. – Termination rates for *t*-butyl radicals in solution ($2k_2$) have been measured by several authors. The reported values in units of $10^9 M^{-1}\,s^{-1}$ were 1.5 (T = 298 K, benzene solvent, [3]), 4.4 (T = 298 K, cyclohexane [3]), 1.8 (T = 298 K, *n*-tridecane [15]), 2.2 (T = 298 K, cyclohexane [15]), 5.4 (T = 298 K, *n*-pentane [15]), 8.1 (T = 298 K, di-*t*-butylperoxide [5]), 11.1 (T = 250 K, isobutane [28]). Our value of $10.2 \cdot 10^9 M^{-1}\,s^{-1}$ at 295 K agrees well with the higher and more recent of these data. We have also redetermined $2k_2$ for benzene solvent and find $2k_2 = 8.2 \cdot 10^9 M^{-1}\,s^{-1}$ slightly higher than our previous value [12]. The general agreement in the order of magnitude for all the solution values puts the much lower value reported for gasphase combination of *t*-butyl [16] in serious question. Since this value was not determined by direct measurement but based on thermochemical parameters of a particular system errors in these parameters may have influenced the result to a large entent.

As has been pointed out by previous authors [3] [5] [15] [28] the order of magnitude of $2k_2$ in solution indicates complete or near diffusion control of the self termination of *t*-butyl. This view is strongly supported by the activation energy of k_2

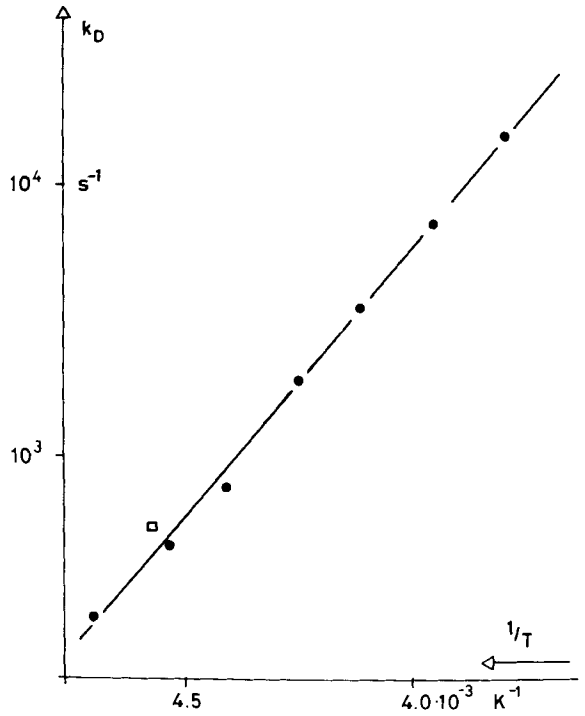

Fig. 9. Arrhennius *plot of* k_D. □: determined from light intensity dependence

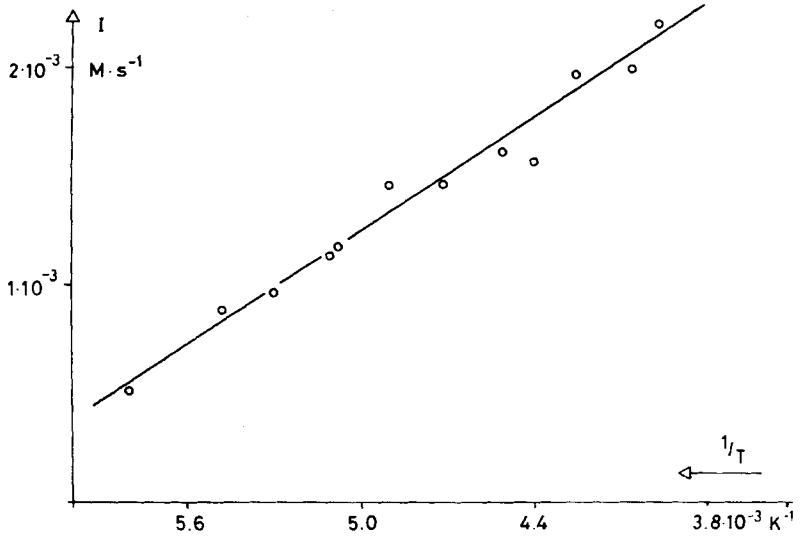

Fig. 10. Arrhennius *plot of I*

which we find to be 2.0 kcal/mol and which is nearly exactly equal to that of the viscosity coefficient of pure methylcyclopentane (1.946 kcal/mol [29]) and methylcyclopentane containing 3% by volume di-*t*-butylketone (2.15 kcal/mol). Our values for $-7.5° \leq T \leq +40°$ (Fig. 8) allow an even more rigorous analysis. From the theory of diffusion controlled reactions in solution [30] we expect $2k_2$ to be given by

$$2k_2 = \sigma \cdot \frac{4\pi D' \cdot \varrho L \cdot 1000^{-1}}{1 + \sigma 4\pi D' \varrho L \cdot 1000^{-1} (2k_\infty)^{-1}} \tag{16}$$

where ϱ is the encounter diameter, D' the relative diffusion coefficient of two radicals, L *Avogadro's* number, and $2k_\infty$ is the rate constant for infinitely fast diffusion. σ is a factor allowing for spin conservation during the reaction. For reactions of two spin uncorrelated radicals it should be $^1/_4$, since only $^1/_4$ of the encounter pairs are in the reactive singlet state. The inclusion of this factor has been discussed for some time, we believe that the success of the recent CIDNP.-theories strongly support its importance [31] [32]. D' is related to the diffusion coefficient of the individual radicals by $D' = 2D$. There are several methods for estimating D from solution data. For radicals larger in size than the solvent molecules the *Stokes-Einstein* equation

$$D = \frac{kT}{6\pi r\eta} \tag{17}$$

should hold where r is the radius of the radical. For small radicals the *Sutherland* modification allowing for sliding friction [33]

$$D = \frac{kT}{4\pi r\eta} \tag{18}$$

should be applicable. Other models have been used by *Hammond* [2] and introduced by *Li et al.* [34]. They all agree in the linear dependence of D on T/η

$$D = C \cdot \frac{T}{\eta} \tag{19}$$

and differ in the expressions for the geometrical factor C. Insertion of the general relation (19) into (16) leads to

$$\frac{1}{2k_2} = A \cdot \frac{\eta}{T} + \frac{1}{2k_\infty} \tag{20}$$

where

$$A = \frac{1000}{\sigma \cdot 8\pi C\varrho \cdot L} \tag{21}$$

Equation (20) shows that $(2k_2)^{-1}$ should depend linearly on η/T, the ordinate for $\eta/T = 0$ giving $(2k_\infty)^{-1}$, if the reaction is nearly diffusion controlled. In Fig. 11 we have plotted averages of rate constants $2k_2$ measured in narrow temperature intervals (Fig. 8) according to Eq. (20) versus η/T for pure solvent [29]. The agreement between predicted and observed behaviour is excellent. The same result is obtained if the solution viscosity is used. The full symbols in Fig. 11 represent values measured for isobutane [28] and benzene solvent. Within experimental error they agree with those for methylcyclopentane solutions. This shows that radical solvent interactions [2] [35] do not influence the reaction rate constant of *t*-butyl, if they are at all present.

From the slope of the straight line we obtain $A = 4.5 \cdot 10^{-6}$ M s KP^{-1}. This quantity is calculated from (18) and (21) with $\sigma = {}^1/_4$ and $\varrho = 2r$ as $A = 12.0 \cdot 10^{-6}$ M s KP^{-1}. If σ is taken to be unity one obtains $A = 3 \cdot 10^{-6}$ M s KP^{-1}. Regarding the idealizations in the derivations of (16) and (18) we consider the agreement between experiment and theory very good, but do not think that our analysis can be used to support or critizise one or the other model.

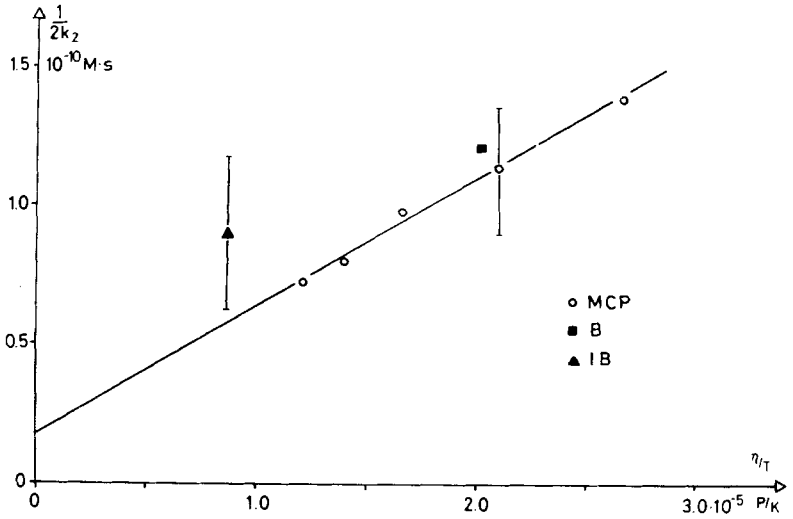

Fig. 11. $(2k_2)^{-1}$ *versus* η/T

From the intercept the rate constant for infinitely fast diffusion $2k_\infty = 5.6 \cdot 10^{10}$ M^{-1} s^{-1} is obtained. By the collision theory of reactions in liquids [36] this can be related to the average frequency of collisions during one encounter ν and the thickness of the cage wall Δ by

$$2k_\infty = \sigma \cdot 4\pi\varrho^2 \Delta \nu L \cdot 1000^{-1} \tag{22}$$

if a steric factor of unity and zero activation energy are assumed. ν can be estimated from the linear expansion coefficient α_1 of the solution [36]. For $\varrho = 2r$ and $\Delta = \varrho$ we obtain

$$2k_\infty = \sigma \cdot 6L\varrho^2 \left(\frac{\pi R}{M \cdot T}\right)^{1/2} \cdot 1000^{-1} \cdot \alpha^{-1} \tag{23}$$

where M is the molecular weight of the radical. Estimating α_1 from the temperature coefficient of the density and assuming $\varrho = 5$ Å and $\sigma = {}^1/_4$ we derive from (23) $2k_\infty = 9.5 \cdot 10^{10}$ M^{-1} s^{-1} at room temperature, again in fair agreement with the experimental value.

The self termination of the pivaloyl radical (k_1) shows a larger activation than that of *t*-butyl (k_2) and an unexpectedly large frequency factor. We can at present not offer an explanation for these findings. Since k_1 was obtained by extrapolating k_2 to low temperatures by an *Arrhennius* law the frequency factor of k_1 may be somewhat erroneous. However, extrapolation of k_2 by Eq. (20) leads to the same activation parameters for k_1.

Rate constants for the unimolecular decomposition of acyl radicals $R - \dot{C}O \rightarrow R\cdot + CO$ in the gas phase have been reported by several authors. For R = phenyl *Benson et al.* [37] have estimated log $(k_D/s^{-1}) = 14.6–29.4/\Theta$. For R = methyl log $(k_D/s^{-1}) = 10.4–15.4/\Theta$ and $= 10.3–15.0/\Theta$ have been measured [19] [38], and for R = propyl log $(k_D/s^{-1}) = 12.8–14.4/\Theta$ [20] and $= 13.3–14.7/\Theta$ [39] were suggested. Comparison of our solution value for R = *t*-butyl log $(k_D/s) = 11.9–9.3/\Theta$ with the literature values shows that all frequency factors are of the expected similar order of magnitude [19], whereas the activation energies vary with the substituent R. In particular the activation energies decrease with increasing stability of the radicals R·. This indicates that the geometry of R· is developed in the transition state, at least to a major extent. The activation energies may also be correlated with the unusual hyperfine parameters of acyl radicals reported previously [10]. Finally, the rate of initiation I, *i.e.* the *Norrish* type I cleavage of the excited ketone (1) shows a small activation energy of 1.2 kcal/mol. This compares well with the similar findings for other ketones [10].

We gratefully acknowledge financial support by the *Swiss National Foundation for Scientific Research.*

REFERENCES

[1] 'Free Radicals', ed. *J. K. Kochi*, Wiley, New York (1973), Vol. I, p. 37ff; Vol. II, p. 475ff; and references cited therein.
[2] *G. S. Hammond, E. J. Hamilton, Jr., S. A. Weiner, H. J. Hefter & A. Gupta*, XXIII Int. Congr. pure appl. Chemistry, Boston, (1971), Spec. Lect. Vol. 4, 257.
[3] *S. A. Weiner & G. S. Hammond*, J. Amer. chem. Soc. *91*, 986 (1969).
[4] *H. J. Hefter, C.-H. S. Wu & G. S. Hammond*, J. Amer. chem. Soc. *95*, 851 (1973).
[5] *G. B. Watts & K. U. Ingold*, J. Amer. chem. Soc. *94*, 491 (1972).
[6] *P. B. Ayscough & M. C. Brice*, J. chem. Soc. B 491 (1971).
[7] *K. Y. Choo & P. P. Gaspar*, J. Amer. chem. Soc. *96*, 1284 (1974).
[8] *E. J. Hamilton, Jr., D. E. Wood & G. S. Hammond*, Rev. scient. Instr. *41*, 452 (1970).
[9] *R. Livingston & H. Zeldes*, J. chem. Physics *59*, 4891 (1973).
[10] *H. Paul & H. Fischer*, Helv. *56*, 1575 (1973).
[11] *H. Paul & H. Fischer*, Chem. Commun. 1038 (1971).
[12] *E. J. Hamilton, Jr. & H. Fischer*, J. phys. Chemistry *77*, 722 (1973).
[13] *N. C. Yang, E. D. Feit, M. H. Hui, N. J. Turro & J. C. Dalton*, J. Amer. chem. Soc. *92*, 6974 (1970).
[14] *B. Blank, A. Henne & H. Fischer*, Helv. *57*, 920 (1974).
[15] *D. J. Carlsson & K. U. Ingold*, J. Amer. chem. Soc. *90*, 7047 (1968).
[16] *R. Hiatt & S. W. Benson*, Int. J. chem. Kinetics *5*, 385 (1973).
[17] *D. E. Applequist & L. Kaplan*, J. Amer. chem. Soc. *87*, 2194 (1965).
[18] *J. A. Kerr & A. C. Lloyd*, Quart. Rev. *22*, 549 (1968).
[19] *H. M. Frey & I. C. Vinall*, Int. J. chem. Kinetics *5*, 523 (1973).
[20] *K. W. Watkins & W. W. Thomson*, Int. J. chem. Kinetics *5*, 791 (1973).
[21] *M. Tomkiewicz, A. Groen & M. Cocivera*, Chem. Physics Letters *10*, 39 (1971).
[22] *H. E. Chien, S. R. Vaich & M. Cocivera*, Chem. Physics Letters *22*, 576 (1973).
[23] *J. W. Kraus & J. G. Calvert*, J. Amer. chem. Soc. *79*, 5921 (1957).
[24] *J. A. G. Dominguez, J. A. Kerr & A. F. Trotman-Dickenson*, J. chem. Soc. 3357 (1962).
[25] *J. A. Kerr & A. F. Trotman-Dickenson*, Progr. React. Kinetics *1*, 107 (1961).
[26] *R. W. Fessenden*, J. chem. Physics *58*, 2489 (1973).
[27] *N. C. Verma & R. W. Fessenden*, J. chem. Physics *58*, 2501 (1973).
[28] *J. E. Bennett, J. A. Eyre, C. P. Rimmer & R. Summers*, Chem. Physics Letters *26*, 69 (1974).
[29] Landolt-Börnstein, Numerical values and Functions, Vol. II, *5*, Part a, Springer-Verlag (1969).

[30] *I. D. Clark & R. P. Wayne*, in 'Comprehensive Chemical Kinetics', ed. C. H. Bamford & C. F. H. Tipper, Elsevier (1969).
[31] 'Free Radicals', ed. J. K. Kochi, Wiley, New York (1973), Vol. I, p. 179.
[32] *R. Kaptein*, J. Amer. chem. Soc. *94*, 6251 (1972).
[33] *G. B. B. M. Sutherland*, Phil. Mag. *9*, 781 (1905).
[34] *J. C. M. Li & P. Chang*, J. chem. Physics *23*, 518 (1955).
[35] *R. D. Burkhart*, J. phys. Chemistry *73*, 2703 (1969).
[36] *A. M. North*, 'Collision Theory of Chemical Reactions in Liquids', Methuen (1964).
[37] *R. K. Solly & S. W. Benson*, J. Amer. chem. Soc. *93*, 2127 (1971).
[38] *H. E. O'Neal & S. W. Benson*, J. chem. Physics *36*, 2196 (1962).
[39] *J. A. Kerr & A. C. Lloyd*, Trans. Farad. Soc. *63*, 2480 (1967).

---

218. Neue Derivate der 7-Amino-cephalosporansäure. Über die Substitution der Acetoxygruppe durch aromatische Reste[1])

Modifikationen von Antibiotica, 11. Mitteilung [1]

von **Heinrich Peter, Hermann Rodriguez, Beat Müller, Walter Sibral** und **Hans Bickel**

Departement Forschung, Division Pharma, *CIBA-GEIGY AG*, Basel

(29. VII. 74)

Summary. 7-Phenylacetamido-3-trifluoroacetoxymethyl-ceph-2-em-4-carboxylic acid (**7**), which is easily produced from the *iso*-cephalosporanic acid derivatives **4** or **6** by treatment with trifluoroacetic acid, reacts smoothly with 'C-nucleophiles' to give derivatives of type **5** (*Schema 1 and 2*). Compounds **5** are converted into microbiologically active cephalosporins of type **8** (Table) by previously described methods.

Die Benzhydrylestergruppe wird in der Chemie der Cephalosporine wegen ihrer leichten Einführbarkeit mit Diphenyldiazomethan und ihrer guten Entfernbarkeit mit Trifluoressigsäure oft als Schutzgruppe verwendet[2]). Die Abspaltung mit Trifluoressigsäure erfolgt meistens in Gegenwart von Anisol, wobei der Diphenylmethylrest in Form von Anisyldiphenylmethan abgefangen wird [2].

Die Anwendung dieser Spaltungsmethode auf Cephalosporansäurederivate der *iso*-Reihe, d.h. auf 3-Acetoxymethyl-Δ^2-cephem-Derivate, führte zu unerwarteten Produkten. Beispielsweise lieferte der Benzhydrylester **4** [R' = $CH(C_6H_5)_2$] bei der Einwirkung von Trifluoressigsäure/Anisol bei Raumtemperatur in wenigen Minuten in über 80% Ausbeute ein Gemisch der Anisylderivate **5a** und **5b** (*Schema 1*), in welchem das *para*-Isomere **a** stark überwog. Vergleichsweise entstehen aus der analogen Δ^3-Verbindung **1** unter denselben Bedingungen nahezu quantitativ die erwartete Säure **2** sowie Anisyldiphenylmethan (**3**).

Den ausserordentlich leicht erfolgenden Austausch der Acetoxygruppe mit dem Anisylrest erklärten wir uns mit der Annahme eines intermediär auftretenden Carboniumions, dessen Bildung bei *iso*-Cephalosporansäurederivaten durch die vinyloge

---

[1]) Auszugsweise vorgetragen an der 'Eleventh Interscience Conference on Antimicrobial Agents and Chemotherapy', Atlantic City, N.J.; 19.–20. Oktober 1971. Vgl. DT OLS 2'132'883.

[2]) Vgl. Patente No. DT 1'445'615 (*Ciba AG*) und DT 1'545'704 (*Ciba AG*).